Diffusion MRI of the Human Brain at Ultra-High Field (UHF): A review

Daniel Gallichan[1]

1. *Cardiff University Brain Research Imaging Centre (CUBRIC), School of Engineering, Cardiff University, Cardiff, UK*

Keywords

Diffusion MRI, ultra-high field, SNR efficiency, simultaneous multi-slice

Word Count: 5724

Abstract

The continued drive towards MRI scanners operating at increasingly higher main magnetic fields is primarily motivated by the maxim that more teslas mean more signal and lead to better images. This promise of increased signal, which cannot easily be achieved in other ways, encourages efforts to overcome the inextricable technical challenges which accompany this endeavor. Unlike for many applications, however, diffusion imaging is not currently able to directly reap these potential signal gains – at the time of writing it seems fair to say that, for matched gradient and RF hardware, the majority of diffusion images acquired at 7T, while comparable in quality to those achievable at 3T, do not demonstrate a clear advantage over what can be obtained at lower field. This does not mean that diffusion imaging at UHF is not a worthwhile pursuit – but more a reflection of the fact that the associated challenges are manifold – and converting the potential of higher field strengths into 'better' diffusion imaging is by no means a straightforward task. This article attempts to summarize the specific reasons that make diffusion imaging at UHF more complicated than one might expect, and to highlight the range of developments that have already been made which have enabled diffusion images of excellent quality to be acquired at 7T.

Introduction and overview

This manuscript explores the difficulties which arise when attempting to perform diffusion imaging of the brain at UHF (or more specifically at 7T, as at the time of writing no examples were found in the literature demonstrating diffusion imaging at field strengths greater than 7T), and examines various approaches that have been put forward to address some of these challenges. 7T MRI is often presented as being capable of providing blanket improvements to all MR sequences, whereas the sobering reality, as is often the case in the parameter-rich field of MR physics, is that of compromises. This is especially true for diffusion imaging, where several of the physical parameters which change with increasing field strength confound to create a rather complex answer to an apparently simple question: is diffusion imaging better at 7T?

The body of this review is split into 5 sections – the first 3 of which exploring different categories of challenges for diffusion imaging at 7T and potential solutions which have been presented in the literature:

1. *The SNR problem for diffusion at UHF*

   Although the intrinsic SNR of the MR signal increases approximately linearly with field strength, the shorter T2 values can cancel out this advantage – especially for diffusion imaging where long echo times are typically used. This section looks at investigations into this relationship, attempting to identify under which regimes 7T can be expected to still deliver a net gain over lower field strengths.

2. *B1-related challenges*

   Increased field strength leads to greater B1-inhomogeneity (due to the shorter RF wavelength) and tighter restrictions due to specific absorption rate (SAR) limits (due to the higher RF energy required to achieve the same flip angle). Both of these changes pose a particular problem for diffusion imaging as a typical diffusion sequence is spin-echo based – where a homogeneous 180° (i.e. high energy) refocusing pulse is highly desirable.

3. *B0-related challenges*

   B0-inhomogeneity is also increased at higher field strengths – which is a particular problem for diffusion imaging as the readout is typically using EPI, which can be severely distorted in the phase-encoding direction at 7T. Shorter T2* values also lead to increased T2-related blurring due to decay occurring during the readout itself.

The final 2 sections look at other developments which do not fit directly into the 3 categories above:

4. *SMS for diffusion at UHF*

   Simultaneous multi-slice (SMS) excitation earns its own category for its potential to increase the capabilities of diffusion imaging at 7T as a result of the acceleration that it provides being essentially at no 'cost' to the user in terms of SNR, as reflected by its rapid widespread uptake for diffusion imaging at 3T. Translating the benefits already demonstrated at 3T up to 7T also presents technical challenges, however, primarily due to SAR constraints and the effect of B1-inhomogeneities on the multi-band pulse.

5. Next generation diffusion imaging at UHF

This section attempts to summarize important work which falls outside the other categories, especially concerning technical improvements that have been demonstrated but not yet applied specifically to diffusion at UHF.

While the choice of distinct categories may give the impression that each of the challenges mentioned may be tackled individually, there are of course many interdependencies which need to be considered when optimizing the sequence as a whole – and therein lies the need for compromise.

1. The SNR problem for diffusion at UHF

When everything else remains equal, the SNR increases approximately linearly with field strength - meaning that moving from 3T to 7T results in roughly 2.3 times higher SNR - and an image of equivalent SNR can be acquired more than 5 times faster. In reality, of course, everything else does not remain equal - other parameters will also be different - which means that estimation of the expected change in SNR is more complicated. Brain tissues at 7T have a longer T1 and a shorter T2 than at 3T. The longer T1 typically means that TR and/or the flip angle may need to be adjusted, but the T1 changes are small enough that these changes are not usually expected to have a major impact on the SNR. The shorter T2 values, however, can be more problematic - especially for diffusion imaging where it is necessary to use long TE values to be able to have time for the diffusion-encoding gradients.

Ugurbil et al (Uğurbil et al., 2013) performed a simulation that gives an indication of in which situations the SNR of 7T is expected to become superior to that of 3T (See Figure 1). Relative SNR (7T/3T) is plotted vs TE for white matter, with various curves showing different assumed TR and readout bandwidths. The bandwidth is also varied in these

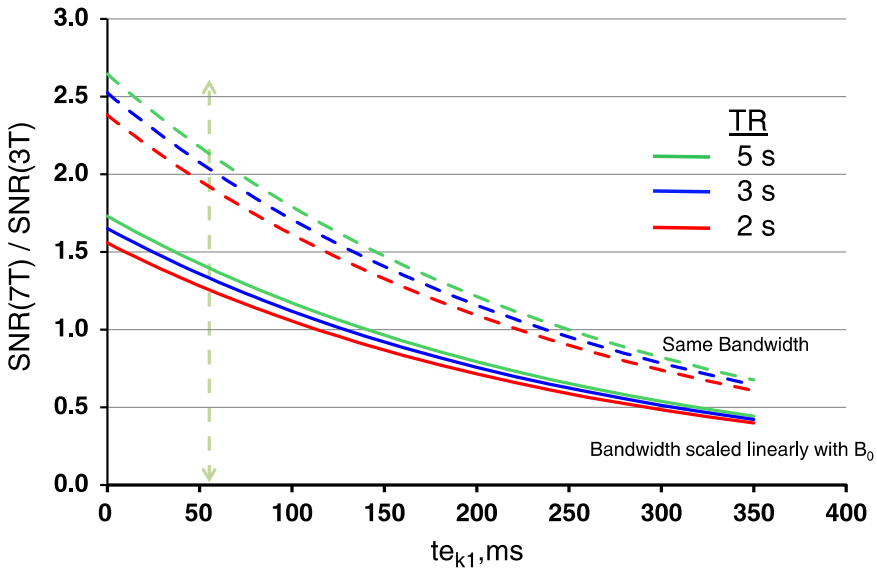

Figure 1. (From (Uğurbil et al., 2013)) Simulated comparison of the expected SNR for a spin-echo sequence at 7T vs 3T as a function of te_{k1}, the time to the first k-space point. The dashed lines show curves where the acquisitions are assumed to have the same bandwidth – and the solid lines assume a higher bandwidth for 7T to compensate for the increased spatial distortions of EPI at higher field.

simulations because of the increased spatial distortions in EPI due to B0 inhomogeneities (see B0 related challenges) when moving to higher field - which often lead to a higher bandwidth being selected at 7T than at 3T to reduce this effect. Overall, however, it is clear that a large SNR gain for 7T over 3T can only be achieved for shorter TE protocols - which means that the largest improvements can be found within the regime of low b-value protocols, or when an exceptionally high performance gradient coil is available for the diffusion encoding. At the time of writing, the maximal gradient strength on clinical 3T systems is in the range 50-80 mT/m depending on the manufacturer - and a small number of research sites have specialized gradients operating at 100 mT/m and even 300 mT/m. As yet it appears that researchers and manufacturers have been hesitant to take on the technical challenges of incorporating such very strong gradient systems into a 7T magnet - a combination which is expected to have the most to offer in terms of SNR for diffusion imaging – with current 7T gradient systems typically operating at 70-80 mT/m.

An experimental comparison of DTI acquisitions at 3T vs 7T was carried out by Choi et al (Choi et al., 2011) where the increased spatial distortions in EPI were offset at 7T by using higher parallel acceleration factors – a strategy that benefits from the reduced g-factors associated with parallel imaging at higher field strengths (Wiesinger et al., 2004). It is also worth noting that for EPI readouts the bandwidth in the phase-encoding direction is often already limited by the gradient hardware, so employing parallel imaging becomes an attractive option to reduce image distortions (see section B0-related challenges) – resulting in a similar effect as the increase in bandwidth in Figure 1. Choi et al showed promising results for 7T, but due to different gradient and RF hardware, as well as restrictions to the 7T sequence due to SAR constraints, it is difficult to make a direct comparison from this data. Comprehensive simulations were performed by Reischauer et al (Reischauer et al., 2012) to compare the SNR at 3T vs 7T – where also the increased spatial distortions at 7T were compensated by increased parallel acceleration. With the specific constraints that were assumed, including a comparatively strong 60% partial Fourier undersampling, 7T was able to offer increased SNR over 3T for smaller voxels sizes and lower acceleration factors. Although for higher acceleration factors 7T could give lower SNR – the acceleration also leads to a smaller point-spread function (PSF) due to the reduced T2-related blurring. A comparison with matched PSF widths would therefore be expected to show a wider parameter range where 7T can demonstrate superior SNR to 3T.

Additionally, the investigation by Reischauer et al (Reischauer et al., 2012) also examined under what circumstances the SNR may be improved by using a stimulated echo (STE) diffusion sequence (Merboldt et al., 1991; Tanner, 1970), where there is potential for a benefit at 7T (Dhital and Turner, 2010). Because the stimulated echo returns magnetization to the longitudinal axis during the diffusion-encoding process, it can outperform a standard spin-echo (SE) sequence in certain conditions – especially when the T2 is short compared with the diffusion time. The direct 50% signal drop associated with using stimulated-echoes, however, means that only under certain conditions will there be a net benefit compared with a spin-echo sequence. Reischauer et al found that at 3T the SE sequence was preferred under all conditions tested, whereas at 7T there can be an SNR advantage for the STE sequence for the combination of high b-values, large voxel size and high parallel acceleration factors. Special care must be taken when attempting DTI with an STE sequence, as the imaging gradients themselves have a greater diffusion-weighting than for the SE sequence – which can in

turn be compensated by appropriate adjustment of the diffusion gradients (Lundell et al., 2014).

A further consideration when evaluating SNR of diffusion sequences is that we can assume that SNR efficiency (SNR of white matter/sqrt(TR)) is optimal for a spin-echo sequence when TR ≈ 1.2 ×T1 (Setsompop et al., 2013). 2D sequences covering the whole-brain typically have TR much longer than this – whereas 3D sequences typically have a TR much shorter. This makes the use of 3D multi-slab acquisitions – which can have a TR much closer to the optimal - particularly attractive when seeking to maximize SNR efficiency (Engström and Skare, 2013; Frost et al., 2014). Excellent quality diffusion images at 1mm isotropic resolution have successfully been acquired at 7T using such an approach (Wu et al., 2016) (see Figure 2). Correspondingly, the SNR efficiency of 2D acquisitions can also be augmented by *reducing* the TR – an additional advantage provided by SMS techniques (*see section SMS for Diffusion at UHF).*

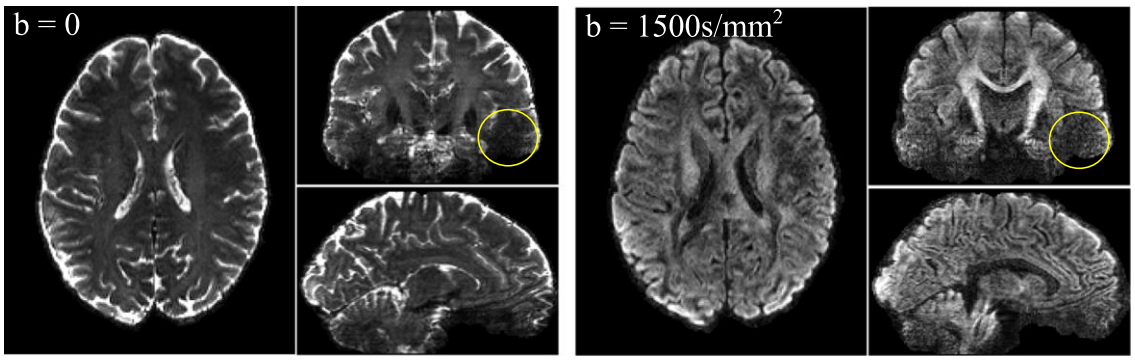

Figure 2: (From (Wu et al., 2016)) High resolution (1mm isotropic) diffusion images acquired at 7T using a 3D multi-slab approach. The yellow circles highlight the region worst affected by signal loss due to B1+ inhomogeneity.

2. B1-related challenges

Diffusion contrast is typically achieved using a spin-echo pulse sequence - primarily due to the need for long diffusion-encoding gradients to achieve the desired degree of diffusion sensitivity, which in turn requires a long echo-time. At such long echo times, the use of a spin-echo can be necessary in order to have sufficient SNR - especially accounting for the additional drop in signal due to the diffusion encoding itself. The reliance of diffusion-sequences on refocusing pulses presents two major challenges when imaging at ultra-high field strengths - the increased difficulty of generating a 'true' 180° pulse across the entire imaging volume (due to the increased B1-inhomogeneities at higher field strengths) and the high energy of refocusing pulses which can easily exceed SAR limitations.

A simple hardware solution to increase the achievable flip-angle in badly affected brain regions is the use of so-called 'dielectric pads' (Haines et al., 2010; Teeuwisse et al., 2012). These are small bags filled with a suspension of high-permittivity material which can be placed adjacent to the head of the subject and significantly alter the shape of the B1+ field. Such dielectric pads have been demonstrated to improve the diffusion signal in low B1+ areas such as the cerebellum and temporal lobe at 7T (Vu et al., 2015), but it should be noted that B1+ homogeneity is not improved across the whole brain.

One approach to improve the homogeneity of the refocusing pulse despite the large B1-inhomogeneities is to use an adiabatic pulse such as in the twice-refocused adiabatic spin echo (TRASE) sequence (Auerbach and Ugurbil, 2004; Skare et al., 2007) (not to be confused with the unrelated method to spatially encode with RF pulses: transmit array spatial encoding, which also adopted the same acronym (Sharp and King, 2010)). As these adiabatic pulses leave a quadratic phase distribution, two of them need to be used in succession in order to allow the phase to be fully refocused. This is not as great a limitation as it may seem, as diffusion protocols at 3T often already use a twice-refocused spin-echo (TRSE) to suppress the effects of eddy-currents resulting from the large diffusion-weighting gradients (Reese et al., 2003). It should be noted, however, that the TRSE approach leads to an increase in TE which reduces SNR due to T2 decay - an effect which is even more pronounced with the shorter T2 values associated with ultra-high field strengths (see previous section).

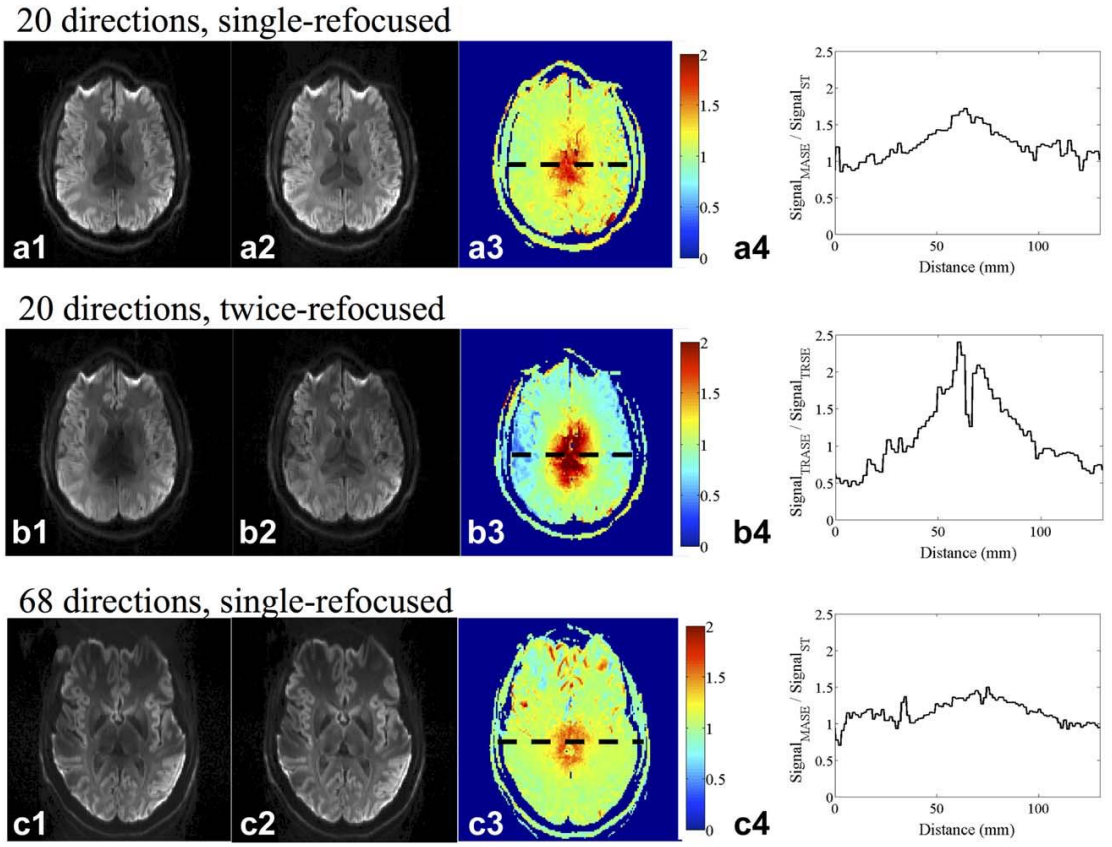

Figure 3. (From (Dyvorne et al., 2016)) Improvements in homogeneity of DWI images acquired at 7T when using adiabatic refocusing pulses. **A1,B1,C1** – conventional refocusing pulses. **A2,B2,C2** adiabatic refocusing (MASE for single-refocusing, TRASE for double-refocusing). **A3,B3,C3** Relative signal adiabatic vs conventional. **A4,B4,C4** – Profiles through center of A3,B3,C3.

Although adiabatic RF pulses can address the problem of B1-inhomogeneity - they are typically associated with an increase in RF power deposition, meaning that SAR restrictions at ultra-high field become an even greater issue. It has recently been demonstrated that it is possible to design semi-adiabatic refocusing pulses which specifically address the problem of B1-inhomogeneity at ultra-high field (Balchandani and Qiu, 2014) - allowing to trade-off some of the adiabaticity in exchange for lower

peak B1 and SAR. Even with these improvements, the SAR threshold can remain restrictive at ultra-high field when two semi-adiabatic pulses are required per readout. Given these SAR limitations, as well as the additional SNR-loss associated with the longer TE of the twice-refocused sequence, it typically proves beneficial to forgo the reduced eddy-currents and return to a single-refocused sequence. It is possible to use a single adiabatic refocusing pulse - provided the excitation pulse is also modified to create a 'matched' phase distribution which cancels the nonlinear phase of the refocusing pulse. Such a matched-phase adiabatic spin-echo (MASE) has been developed and demonstrated in vivo at 7T (Dyvorne et al., 2016). Figure 3 shows examples of improvements in signal homogeneity achievable through TRASE and MASE.For many MR imaging techniques it is possible to improve the poor homogeneity of the RF excitation at ultra-high field strengths without needing to use adiabatic pulses, but instead by modifying the RF transmission process. If suitable hardware is available, multiple channels of the RF transmit system can be adjusted separately to have an individually chosen amplitude and phase (RF shimming) - but a large number of transmit channels are required to achieve good homogeneity, with 16-channels providing a homogeneous whole-brain shim at 7T, and more channels being necessary at even higher fields (Mao et al., 2006). Composite RF pulses, even as simple as two consecutive 90 degree pulses with a 90 degree phase shift between them, have also been shown to reduce RF transmit inhomogeneities (Thesen et al., 2003) - an approach which can also be combined with RF shimming to get even better homogeneity (Collins et al., 2007). Alternatively, the RF pulse can be combined with gradient waveforms in order to traverse the transmission k-space (Pauly, 1989) thereby creating a 'shaped' excitation profile which can counteract the known inhomogeneities of the transmit field. Such pulses are inherently much longer in duration than standard RF pulses, but they can be shortened by parallel acceleration (i.e. 'transmit SENSE' - requiring hardware where the individual RF transmit channels can deliver independent waveforms (Katscher et al., 2003)) or by selecting only a few 'points' in the transmit k-space which are covered (Cloos et al., 2012).

Overall a large number of methods exist to tailor the RF transmission process - but most of them have yet to be demonstrated in application to diffusion imaging. Many of the advances in parallel transmission are based on the small tip-angle regime, and therefore they can be difficult to translate into the large flip angles required for diffusion imaging. Additionally, not only must suitable hardware be available to perform the parallel transmission - and also ideally combined with a high channel-count receive RF array to maintain SNR - but the system also needs to have a highly-trusted SAR model to be able to transmit on multiple channels at high energy (*see separate review on parallel transmission in this issue)*.

An additional consideration for diffusion imaging at UHF is the increased difficulty of achieving good fat suppression using the conventional approach of a spectrally selective fat suppression pulse before each excitation – as this adds additional SAR exposure to the sequence and the quality of the fat suppression can be degraded to B1+ inhomogeneities. Several recent studies(Heidemann et al., 2010; Strotmann et al., 2014; Vu et al., 2015) report having been able to achieve good fat suppression with no SAR penalty for diffusion imaging at 7T by using the method of Ivanov et al (Ivanov et al., 2010) which involves using different bandwidths for the excitation and refocusing RF pulses in the spin-echo acquisition such that the fat signal does not get refocused, and

can even be combined with gradient reversal techniques (Park et al., 1987) to avoid increasing TE (Heidemann et al., 2010).

3. B0-related challenges

A further consequence of the long readout duration associated with EPI is a high propensity for image distortions in the phase-encoding direction due to variations in the B0-field. At ultra-high field strengths this problem is particularly acute as the B0-field variations induced by susceptibility changes between tissues and air spaces around the head scale with the main magnetic field. EPI readouts are also sensitive to blurring due to T2-related decay during the extended readout duration but, as spin-echo EPI is typically employed for diffusion acquisitions rather than gradient-echo, this effect is mitigated by the symmetry of the resulting weighting function in k-space. Often referred to in the literature as T2* blurring, for a spin-echo the effect is actually dependent on the difference between T2* and T2 as well as the T2 itself. Regardless of nomenclature, it has been demonstrated that the T2-related blurring can be clearly observed in diffusion sequences at 7T (Heidemann et al., 2010)

A variety of methods exist to correct for susceptibility-induced distortions, e.g. (Andersson et al., 2003; Chen and Wyrwicz, 1999; Jezzard and Balaban, 1995), but large distortions will inevitably continue to have a detrimental effect on the image quality, even after such corrections. The effects of distortions can be mitigated by increasing the rate of k-space traversal, which can be achieved in three main ways (besides simply increasing the readout bandwidth): segmenting the acquisition into multiple shots (Atkinson et al., 2000; Butts et al., 1997; Holdsworth et al., 2008; Nunes et al., 2005; Porter and Heidemann, 2009; Robson et al., 1997); skipping lines of k-space and filling them using parallel acceleration techniques (such as SENSE (Pruessmann et al., 1999) or GRAPPA (Griswold et al., 2002)) or by reduced-FOV techniques (Feinberg et al., 1985; Heidemann et al., 2012; Mansfield et al., 1988; Rieseberg et al., 2002; Wilm et al., 2007). All three techniques can be used together in the same acquisition protocol if desired. It should be noted that although partial Fourier undersampling does also reduce the length of the readout, it is the rate of k-space traversal which determines the extent of image distortions and T2-related blurring - and this remains the same when the typical ¾ partial Fourier undersampling is applied in the EPI blip-encoding direction. For diffusion imaging, partial Fourier undersampling may be employed as a method to reduce the TE, but it does not reduce distortions or blurring.

All three of the approaches listed above for shortening the EPI readout have the additional advantage, just like partial Fourier undersampling, of reaching the center of k-space sooner - thereby reducing the TE and reducing the signal loss due to T2 decay. This dual benefit of shortening the readout - most readily achieved through parallel imaging - has meant that the recent advances in RF coil design, and increased availability of high-channel count receive arrays, have been particularly significant for UHF diffusion imaging. Indeed, high-quality high-resolution diffusion-weighted images have been acquired at 7T using a combination of SENSE and segmentation (Jeong et al., 2013); GRAPPA and segmentation in the readout direction (Heidemann et al., 2010); SENSE with reduced-FOV imaging (von Morze et al., 2010; Wargo and Gore, 2013) or by using GRAPPA with zoomed-imaging (referred to as ZOOmed imaging and Partially Parallel Acquisition - (Heidemann et al., 2012)).

The high sensitivity of EPI to B0-inhomogeneities can mean that alternative readouts might also become a preferred option for certain applications at ultra-high field strengths. The single-shot rapid acquisition with relaxation enhancement (RARE) readout (Hennig et al., 1986), where each line of k-space is acquired with its own spin-echo, does not suffer from the same distortions and dropout as are associated with EPI - but it is does typically lead to longer total readout durations and increased SAR deposition. RARE can be a good choice for diffusion-sensitized ophthalmic imaging ((Paul et al., 2015) – see Figure 4) where b-values are relatively low (300 s/mm^2 in (Paul et al., 2015)) and where minimizing distortions is of paramount importance for the application - and feasibility of using RARE for DTI at 7T has also been demonstrated (Sigmund and Gutman, 2011).

4. SMS for diffusion at UHF

In recent years there has been widespread use of simultaneous multi-slice (SMS) acquisitions (Breuer et al., 2005; Feinberg et al., 2010; Larkman et al., 2001; Moeller et al., 2010; K. Setsompop et al., 2012; Kawin Setsompop et al., 2012) (*see also review article in this special issue)*, primarily for fMRI and DTI applications. The benefits of using SMS are particularly clear for diffusion-weighted imaging, as the majority of the time during the scan is allocated to the long diffusion preparation when high b-values are being acquired. If more of the imaging volume can be excited and spatially-encoded for each set of diffusion-encoding gradients, the scan will become more efficient. In other imaging applications this can often be achieved simply by switching from a multi-slice 2D acquisition to a full 3D acquisition with two phase-encoding directions (Narsude et al., 2014; Poser et al., 2010) – which also means using a multi-shot acquisition due to the long readout times associated with covering a full 3D k-space. Although this is also possible for diffusion-weighted imaging, it typically becomes complicated to deal with the phase inconsistencies resulting from multi-shot sequences - as differential tissue movement during the acquisition of each shot will impart differential phase information following the diffusion-encoding gradients. Phase inconsistencies for multi-shot 2D sequences can be compensated by the use of 2D-navigators (Atkinson et al., 2000; Butts et al., 1997; Miller and Pauly, 2003), but more complex navigators are necessary to capture 3D phase information (McNab et al., 2010; O'Halloran et al., 2013).

The SMS approach is able to avoid the need for phase-navigators by effectively being a hybrid between 2D and 3D spatial encoding - several slices are excited together and can be read out in a single shot - thereby avoiding the need for a navigator. The separation of the data from the simultaneously acquired slices is achieved by parallel imaging. This means that, compared to 2D multi-slice experiments, SMS reduces the TR by a factor equal to the multi-band factor (i.e. the number of simultaneously acquired slices), shortening the overall scan-time by the same factor and with minimal SNR penalty. This is completely unlike a conventional SENSE or GRAPPA acceleration, which for a simple GRE acquisition with acceleration factor R will be acquired R-times faster, but with an SNR penalty of at least sqrt(R) - and the additional 'g-factor' which accounts for how well-conditioned the matrix inversion is for the parallel image reconstruction (Pruessmann et al., 1999). For SMS the scan-time can be reduced by the multi-band factor, but this does not reduce SNR because the amount of data which has been

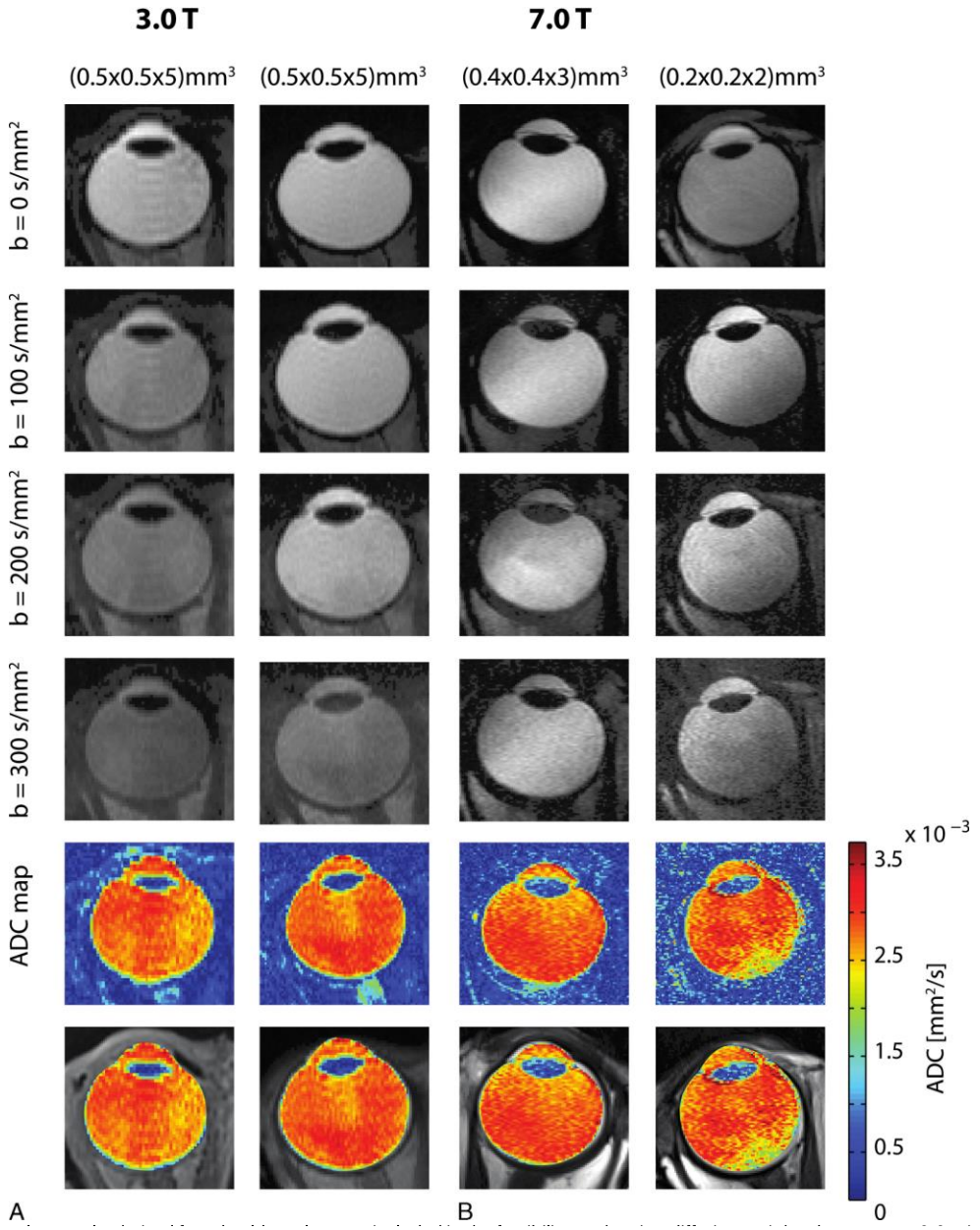

Figure 4. (From Paul 2015) Comparison of image quality possible with an ophthalmic diffusion weighted ms-RARE sequence at (a) 3T vs (b) 7T.

encoded is increased by the same factor - and g-factor losses are minimal when using the blip-controlled aliasing (Kawin Setsompop et al., 2012). There is a slight SNR drop due to the shorter TR, but this is compensated by a net increase in the SNR efficiency as the TR is brought closer to the optimal value of ≈ 1.2 ×T1 for a spin-echo sequence.

The implementation of SMS at ultra-high field strengths can be more problematic due to the associated increase in SAR with the multi-band excitation and refocusing pulses, as well as the increased difficulty of achieving high quality multi-band excitations and refocusing in the presence of increased B1-inhomogeneities. Excellent quality multi-band diffusion images have been acquired at high resolution at 7T using a protocol developed as part of the Human Connectome Project (HCP) (Vu et al., 2015). Interestingly, most diffusion data presented at 7T is acquired at b-values of 1000 s/mm^2 or lower due to SNR concerns from the longer TEs required for high b-values – yet the HCP data show high data quality at b=2000 s/mm^2 even at 7T (Vu et al., 2015).

As a proof-of-concept, SMS has been also successfully demonstrated in combination with readout segmentation at 7T ((Frost et al., 2015)– see Figure 5) - but the overall acceleration was artificially restricted due to the need to insert additional dead-time due to SAR restrictions. The SAR burden associated with SMS can be significantly reduced by using Power Independent of Number of Slices (PINS) RF pulses (Norris et al., 2011) and this has also been demonstrated at 7T for diffusion imaging (Eichner et al., 2014; Koopmans et al., 2015), albeit with the additional constraint that PINS pulses excite a (theoretically) infinite number of simultaneous slices and this must be appropriately compensated for in the sequence design. PINS pulses have also been combined with similar pulse-design approaches to those discussed in the section on B1-related challenges have already been applied to SMS at 7T, resulting in improved B1-

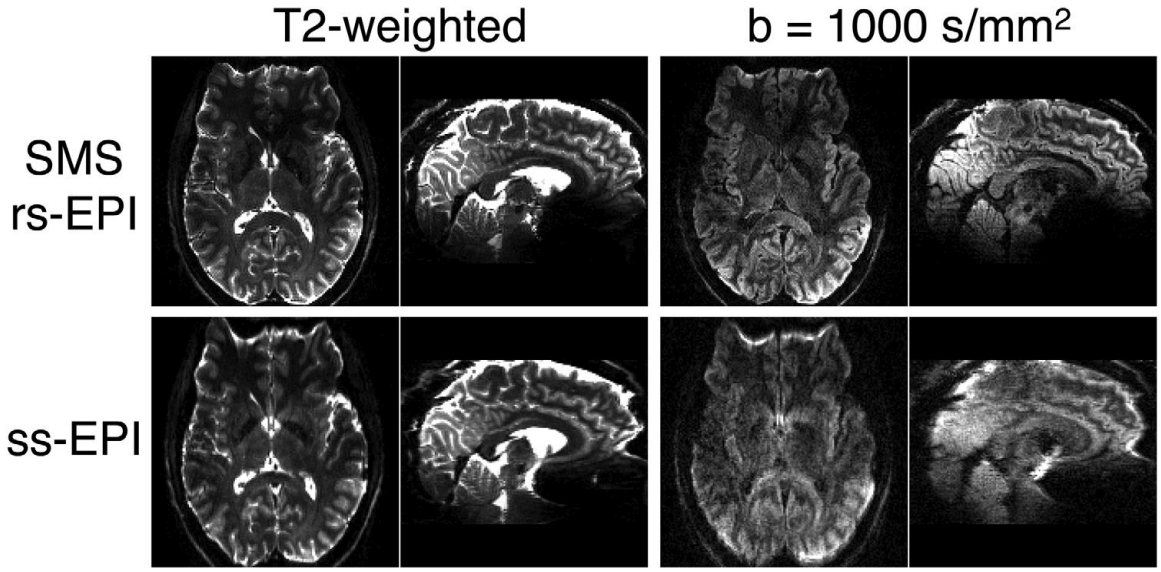

Figure 5. (from Frost 2015) Examples of raw T2-weighted and b=1000 s/mm^2 images acquired at 7T with single-shot EPI (ss-EPI) and SMS readout-segmented EPI (SMS rs-EPI) DTI protocols with 1.2 mm isotropic resolution

immunity as well as lower SAR (Feldman et al., 2016) – and preliminary results have even been presented using multi-band pulses optimized with parallel transmit technology at 7T (Wu et al., 2014).

5. Next generation diffusion imaging at UHF

There have been a number of recent developments in hardware and software that have not yet been applied specifically to diffusion imaging at UHF, but should in theory provide significant benefits. As was discussed in the previous section, increasing the performance of the gradients is one of the most effective ways to improve sensitivity to diffusion making this the most obvious hardware improvement that might also be applied to UHF - and provide a way to get even more diffusion sensitivity from these ultra-strong gradient coils. Given that such gradient systems push the limits of what is achievable from the hardware - as well as encroaching on physiological limits of peripheral nerve and/or cardiac stimulation when they are switched - it is perhaps understandable that so far the challenge of combining ultra-strong gradients with UHF has not yet been taken up.

Recent work has demonstrated the suitability of shim coil arrays to better shim the human brain, either as a dedicated additional array (Juchem et al., 2011) or even by running DC currents for shimming along the same coil elements being used for the RF reception on a specially designed array (Stockmann et al., 2016; Truong et al., 2014) (*see review article in this issue).* Improved shimming could be particularly relevant for diffusion imaging at UHF, as this can counterbalance the increased spatial distortions in EPI when moving to higher fields (see section B0-related challenges). It can also be seen from Figure 1 that the SNR gain moving from 3T to 7T is higher when the bandwidth of the readout is kept the same - and with improved shimming it may be possible to avoid the need to increase the bandwidth, which might typically be done at higher fields to keep the resulting spatial distortions within an acceptable range.

It is now possible to purchase a commercialized version of the MR field probes described in (Barmet et al., 2009) which allow detailed characterization of the spatiotemporal field evolution during an MR experiment. For diffusion imaging such a system could be beneficial in a number of ways. A better characterization of the eddy currents induced by the gradient hardware could mean they can be more accurately corrected in post-processing. This could be particularly relevant for UHF diffusion imaging where the biggest gains are with shorter TEs – which could be facilitated by better characterization of eddy-current effects from very strong gradients, as well as increasing the robustness of non-Cartesian k-space trajectories, such as spirals, that enable shorter TEs. Furthermore, field probes that can remain in position during the scan itself can also be used to track changes in gradient behavior due to slow system drifts, as well as physiologically induced changes in the field - particularly due to breathing (Vannesjo et al., 2015).

Another hardware improvement which also obviously has the potential to further improve diffusion sensitivity is a further increase in the main magnetic field strength. It is clear that there are myriad challenges associated with exploiting the major developments in superconductor materials that have happened in recent years in order

to construct MRI systems at much higher field strengths than have been achieved so far. Despite these challenges, an initiative already exists with researchers from a number of international institutions with the aim of building MRI scanners for human brain imaging in the 14-20 T range (Budinger et al., 2016). Given that, as outlined in this article, there are already many specific challenges associated with diffusion imaging in the currently accessible UHF range (7-9.4T), it is unlikely that diffusion imaging will be a high priority when these systems are built. However, as the technology becomes established we can expect researchers to also begin to investigate how the rich SNR gains of such exceptionally high fields can also be applied to diffusion.

We have already discussed in this article the potential that simultaneous multi-slice (SMS) acquisitions have to offer for diffusion at UHF - and recently this concept has been taken even further by combining it with super-resolution encoding of multiple simultaneously excited imaging slabs, referred to as Slice Dithered Enhanced Resolution SMS (SLIDER-SMS) (Setsompop et al., 2015). So far this technique has only been demonstrated on a 3T MR system with exceptional gradient strength (300 mT/m) to obtain remarkably high resolution (so far down to 660 μm isotropic (Setsompop et al., 2016)) - but we can expect future work will seek to address the additional challenges associated of bringing these advances to UHF (*see review article in this issue)*. Indeed, very high-spatial resolution diffusion imaging is expected to be an application where 7T can outperform lower field strengths – and this has already been exploited using zoomed imaging at 7T to assist in modelling the induced electric field in transcranial magnetic stimulation (Opitz et al., 2011) and for exploring the habenula in vivo (Strotmann et al., 2014).

There have also been significant recent advances in the processing of diffusion data which can, in turn, lead to improvements in diffusion image quality. It has been demonstrated that it can be advantageous to perform the distortion-correction of the EPI images simultaneously with the registration for motion-correction in a single combined correction (Andersson and Sotiropoulos, 2015). This method (available as 'EDDY' in the publically released FSL package - http://fsl.fmrib.ox.ac.uk/fsl/fslwiki) can also directly incorporate correction for the susceptibility-induced distortions at the same time, driven either by a separately acquired B0-map or by including reversal of the phase-encoding direction in the diffusion acquisition itself. As mentioned for the NMR probes above, approaches which can better cope with eddy-currents can be particularly relevant at UHF as eddy currents tend to be a bigger problem at shorter TEs where UHF has the greatest gains.

An interesting example of how diffusion data acquired at 7T can be used to complement data acquired at 3T was recently presented, where publically available data from the WU-Minn HCP (Van Essen et al., 2013) were reprocessed for subjects where diffusion images were acquired at both field strengths (Sotiropoulos et al., 2016). The 3T data were acquired with greater sampling of q-space (90 directions on each of 3 b-value shells at 1.25 mm resolution) and the 7T data were acquired at higher spatial resolution (65 directions on 2 shells at 1.05 mm resolution). A combined data fusion model was then used to estimate fiber orientations at the higher spatial resolution – with greater fidelity than could have been achieved using either dataset on its own. Diffusion imaging at UHF is likely to remain advantageous only within certain imaging regimes – and such

a fusion approach offers an intriguing method to broaden the range of applications where these regimes apply.

Conclusion

As will be clear from this article, the simple question posed in the Introduction ('is diffusion imaging better at 7T?') has no simple answer. In terms of sequences which are already widely available, it is generally possible to produce images of a similar quality to that which users will be familiar with at 3T – but these will typically take longer to acquire due to the increased SAR constraints. This means that 7T would not currently be the field strength of choice for performing a 'standard' DTI study, for example. However, users wishing to run a multi-modal study at UHF should be able to include a diffusion imaging component without needing to have their subjects rescanned at lower field.

From the developments summarized in this article, it is also clear that it is possible to achieve diffusion images of excellent quality at 7T. We can expect clear improvements in applications which allow operating in the 'sweet-spot' of what 7T has to offer – lower b-values (allowing shorter TE and less T2-decay) and at high resolution (where the increased parallel acceleration capability keeps the readout within a feasible duration). This means that even when a robust diffusion sequence is made available for 7T incorporating as many of the latest technical improvements as possible, it is likely to also only be able to offer clear advantages over lower fields when operating in a similar 'sweet spot' regime.

Acknowledgements

The author is exceptionally grateful to Wenchuan Wu for invaluable comments for revising the manuscript and increasing the coverage of important aspects of the relevant literature.

References

Andersson, J.L.R., Skare, S., Ashburner, J., 2003. How to correct susceptibility distortions in spin-echo echo-planar images: application to diffusion tensor imaging. Neuroimage 20, 870–888. doi:10.1016/S1053-8119(03)00336-7

Andersson, J.L.R., Sotiropoulos, S.N., 2015. An integrated approach to correction for off-resonance effects and subject movement in diffusion MR imaging. Neuroimage 125, 1063–1078. doi:10.1016/j.neuroimage.2015.10.019

Atkinson, D., Porter, D.A., Hill, D.L.G., Calamante, F., Connelly, A., 2000. Sampling and reconstruction effects due to motion in diffusion-weighted interleaved echo planar imaging. Magn. Reson. Med. 44, 101–109. doi:10.1002/1522-2594(200007)44:1<101::AID-MRM15>3.0.CO;2-S

Auerbach, E.J., Ugurbil, K., 2004. Improvement in Diffusion MRI at 3T and Beyond with the Twice-Refocused Adiabatic Spin Echo (TRASE) Sequence, in: Proceedings of the 11th Annual Meeting of ISMRM, Kyoto, Japan. p. 2464.

Balchandani, P., Qiu, D., 2014. Semi-adiabatic Shinnar-Le Roux pulses and their application to diffusion tensor imaging of humans at 7T. Magn. Reson. Imaging 32, 804–12. doi:10.1016/j.mri.2014.04.003

Barmet, C., De Zanche, N., Wilm, B.J., Pruessmann, K.P., 2009. A transmit/receive system for magnetic field monitoring of in vivo MRI. Magn Reson Med 62, 269–76. doi:10.1002/mrm.21996

Breuer, F. a, Blaimer, M., Heidemann, R.M., Mueller, M.F., Griswold, M. a, Jakob, P.M., 2005. Controlled aliasing in parallel imaging results in higher acceleration (CAIPIRINHA) for multi-slice imaging. Magn Reson Med 53, 684–91. doi:10.1002/mrm.20401

Budinger, T.F., Bird, M.D., Frydman, L., Long, J.R., Mareci, T.H., Rooney, W.D., Rosen, B., Schenck, J.F., Schepkin, V.D., Sherry, A.D., Sodickson, D.K., Springer, C.S., Thulborn, K.R., U??urbil, K., Wald, L.L., 2016. Toward 20T magnetic resonance for human brain studies: opportunities for discovery and neuroscience rationale. Magn. Reson. Mater. Physics, Biol. Med. 29, 617–639. doi:10.1007/s10334-016-0561-4

Butts, K., Pauly, J., De Crespigny, A., Moseley, M., 1997. Isotropic diffusion-weighted and spiral-navigated interleaved EPI for routine imaging of acute stroke. Magn. Reson. Med. 38, 741–749. doi:10.1002/mrm.1910380510

Chen, N.K., Wyrwicz, a M., 1999. Correction for EPI distortions using multi-echo gradient-echo imaging. Magn Reson Med 41, 1206–13.

Choi, S., Cunningham, D.T., Aguila, F., Corrigan, J.D., Bogner, J., Mysiw, W.J., Knopp, M. V, Schmalbrock, P., 2011. DTI at 7 and 3 T: systematic comparison of SNR and its influence on quantitative metrics. Magn. Reson. Imaging 29, 739–51. doi:10.1016/j.mri.2011.02.009

Cloos, M.A., Boulant, N., Luong, M., Ferrand, G., Giacomini, E., Le Bihan, D., Amadon, A., 2012. K T-points: Short three-dimensional tailored RF pulses for flip-angle homogenization over an extended volume. Magn. Reson. Med. 67, 72–80. doi:10.1002/mrm.22978

Collins, C.M., Wang, Z., Mao, W., Fang, J., Liu, W., Smith, M.B., 2007. Array-optimized composite pulse for excellent whole-brain homogeneity in high-field MRI. Magn. Reson. Med. 57, 470–474. doi:10.1002/mrm.21172

Dhital, B., Turner, R., 2010. Diffusion Weighted Imaging at {7T} with {STEAM-EPI} and {GRAPPA}. Proc. ISMRM 46, 3994.

Dyvorne, H., O'Halloran, R., Balchandani, P., 2016. Ultrahigh field single-refocused diffusion weighted imaging using a matched-phase adiabatic spin echo (MASE). Magn. Reson. Med. 75, 1949–1957. doi:10.1002/mrm.25790

Eichner, C., Setsompop, K., Koopmans, P.J., Lützkendorf, R., Norris, D.G., Turner, R., Wald, L.L., Heidemann, R.M., 2014. Slice accelerated diffusion-weighted imaging at ultra-high field strength. Magn. Reson. Med. 71, 1518–1525. doi:10.1002/mrm.24809

Engström, M., Skare, S., 2013. Diffusion-weighted 3D multislab echo planar imaging for high signal-to-noise ratio efficiency and isotropic image resolution. Magn. Reson.

Med. 70, 1507–1514. doi:10.1002/mrm.24594

Feinberg, D.A., Hoenninger, J.C., Crooks, L.E., Kaufman, L., Watts, J.C., Arakawa, M., 1985. Inner volume MR imaging: technical concepts and their application. Radiology 156, 743–747. doi:10.1148/radiology.156.3.4023236

Feinberg, D.A., Moeller, S., Smith, S.M., Auerbach, E., Ramanna, S., Glasser, M.F., Miller, K.L., Ugurbil, K., Yacoub, E., 2010. Multiplexed echo planar imaging for sub-second whole brain FMRI and fast diffusion imaging. PLoS One 5, e15710. doi:10.1371/journal.pone.0015710

Feldman, R.E., Islam, H.M., Xu, J., Balchandani, P., 2016. A SEmi-Adiabatic matched-phase spin echo (SEAMS) PINS pulse-pair for B 1 -insensitive simultaneous multislice imaging. Magn. Reson. Med. 75, 709–717. doi:10.1002/mrm.25654

Frost, R., Jezzard, P., Douaud, G.G., Clare, S., Porter, D.A., Miller, K.L., 2015. Scan time reduction for readout-segmented EPI using simultaneous multislice acceleration: Diffusion-weighted imaging at 3 and 7 Tesla. Magn. Reson. Med. 74, 136–149. doi:10.1002/mrm.25391

Frost, R., Miller, K.L., Tijssen, R.H.N., Porter, D.A., Jezzard, P., 2014. 3D Multi-slab diffusion-weighted readout-segmented EPI with real-time cardiac-reordered k-space acquisition. Magn. Reson. Med. 72, 1565–1579. doi:10.1002/mrm.25062

Griswold, M.A., Jakob, P.M., Heidemann, R.M., Nittka, M., Jellus, V., Wang, J., Kiefer, B., Haase, A., 2002. Generalized autocalibrating partially parallel acquisitions (GRAPPA). Magn Reson Med 47, 1202–1210. doi:10.1002/mrm.10171

Haines, K., Smith, N.B., Webb, A.G., 2010. New high dielectric constant materials for tailoring the B1+ distribution at high magnetic fields. J. Magn. Reson. 203, 323–327. doi:10.1016/j.jmr.2010.01.003

Heidemann, R.M., Anwander, A., Feiweier, T., Knösche, T.R., Turner, R., 2012. k-space and q-space: combining ultra-high spatial and angular resolution in diffusion imaging using ZOOPPA at 7 T. Neuroimage 60, 967–78. doi:10.1016/j.neuroimage.2011.12.081

Heidemann, R.M., Porter, D. a, Anwander, A., Feiweier, T., Heberlein, K., Knösche, T.R., Turner, R., 2010. Diffusion imaging in humans at 7T using readout-segmented EPI and GRAPPA. Magn Reson Med 64, 9–14. doi:10.1002/mrm.22480

Hennig, J., Nauerth, A., Friedburg, H., 1986. RARE imaging: a fast imaging method for clinical MR. Magn Reson Med 3, 823–33.

Holdsworth, S.J., Skare, S., Newbould, R.D., Guzmann, R., Blevins, N.H., Bammer, R., 2008. Readout-segmented EPI for rapid high resolution diffusion imaging at 3 T. Eur. J. Radiol. 65, 36–46. doi:10.1016/j.ejrad.2007.09.016

Ivanov, D., Schäfer, A., Streicher, M.N., Heidemann, R.M., Trampel, R., Turner, R., 2010. A simple low-SAR technique for chemical-shift selection with high-field spin-echo imaging. Magn. Reson. Med. 64, 319–326. doi:10.1002/mrm.22518

Jeong, H.-K., Gore, J.C., Anderson, A.W., 2013. High-resolution human diffusion tensor

imaging using 2-D navigated multishot SENSE EPI at 7 T. Magn. Reson. Med. 69, 793–802. doi:10.1002/mrm.24320

Jezzard, P., Balaban, R.S., 1995. Correction for geometric distortion in echo planar images from B0 field variations. Magn Reson Med 34, 65–73.

Juchem, C., Nixon, T.W., McIntyre, S., Boer, V.O., Rothman, D.L., De Graaf, R.A., 2011. Dynamic multi-coil shimming of the human brain at 7 T. J. Magn. Reson. 212, 280–288. doi:10.1016/j.jmr.2011.07.005

Katscher, U., Börnert, P., Leussler, C., Van den Brink, J.S., 2003. Transmit SENSE. Magn. Reson. Med. 49, 144–150. doi:10.1002/mrm.10353

Koopmans, P.J., Frost, R., Porter, D.A., Wu, W., Jezzard, P., Miller, K.L., Barth, M., 2015. Diffusion-Weighted Readout-Segmented EPI Using PINS Simultaneous Multislice Imaging Peter, in: Proceedings of the 23rd Annual Meeting of the ISMRM, Toronto, Canada. p. 959.

Larkman, D.J., Hajnal, J. V., Herlihy, A.H., Coutts, G.A., Young, I.R., Ehnholm, G., 2001. Use of multicoil arrays for separation of signal from multiple slices simultaneously excited. J. Magn. Reson. Imaging 13, 313–317. doi:10.1002/1522-2586(200102)13:2<313::AID-JMRI1045>3.0.CO;2-W

Lundell, H., Alexander, D.C., Dyrby, T.B., 2014. High angular resolution diffusion imaging with stimulated echoes: Compensation and correction in experiment design and analysis. NMR Biomed. 27, 918–925. doi:10.1002/nbm.3137

Mansfield, P., Ordidge, R.J., Coxon, R., 1988. Zonally magnified EPI in real time by NMR. J. Phys. E. 21, 275. doi:10.1088/0022-3735/21/3/008

Mao, W., Smith, M.B., Collins, C.M., 2006. Exploring the limits of RF shimming for high-field MRI of the human head. Magn. Reson. Med. 56, 918–922. doi:10.1002/mrm.21013

McNab, J.A., Gallichan, D., Miller, K.L., 2010. 3D steady-state diffusion-weighted imaging with trajectory using radially batched internal navigator echoes (TURBINE). Magn Reson Med 63, 235–42. doi:10.1002/mrm.22183

Merboldt, K.D., Hänicke, W., Frahm, J., 1991. Diffusion imaging using stimulated echoes. Magn. Reson. Med. 19, 233–9. doi:10.1002/mrm.1910190208

Miller, K.L., Pauly, J.M., 2003. Nonlinear phase correction for navigated diffusion imaging. Magn Reson Med 50, 343–53. doi:10.1002/mrm.10531

Moeller, S., Yacoub, E., Olman, C. a, Auerbach, E., Strupp, J., Harel, N., Uğurbil, K., 2010. Multiband multislice GE-EPI at 7 tesla, with 16-fold acceleration using partial parallel imaging with application to high spatial and temporal whole-brain fMRI. Magn Reson Med 63, 1144–53. doi:10.1002/mrm.22361

Narsude, M., Van Der Zwaag, W., Kober, T., Gruetter, R., Marques, J.P., 2014. Improved temporal resolution for functional studies with reduced number of segments with three-dimensional echo planar imaging. Magn. Reson. Med. 72, 786–792. doi:10.1002/mrm.24975

Norris, D.G., Koopmans, P.J., Boyacioğlu, R., Barth, M., 2011. Power Independent of Number of Slices (PINS) radiofrequency pulses for low-power simultaneous multislice excitation. Magn. Reson. Med. 66, 1234–40. doi:10.1002/mrm.23152

Nunes, R.G., Jezzard, P., Behrens, T.E.J., Clare, S., 2005. Self-navigated multishot echo-planar pulse sequence for high-resolution diffusion-weighted imaging. Magn. Reson. Med. 53, 1474–1478. doi:10.1002/mrm.20499

O'Halloran, R.L., Aksoy, M., Van, A.T., Bammer, R., 2013. 3D isotropic high-resolution diffusion-weighted MRI of the whole brain with a motion-corrected steady-state free precession sequence. Magn. Reson. Med. 70, 466–478. doi:10.1002/mrm.24489

Opitz, A., Windhoff, M., Heidemann, R.M., Turner, R., Thielscher, A., 2011. How the brain tissue shapes the electric field induced by transcranial magnetic stimulation. Neuroimage 58, 849–859. doi:10.1016/j.neuroimage.2011.06.069

Park, H.W., Kim, D.J., Cho, Z.H., 1987. Gradient reversal technique and its applications to chemical???shift???related NMR imaging. Magn. Reson. Med. 4, 526–536. doi:10.1002/mrm.1910040604

Paul, K., Graessl, A., Rieger, J., Lysiak, D., Huelnhagen, T., Winter, L., Heidemann, R., Lindner, T., Hadlich, S., Zimpfer, A., Pohlmann, A., Endemann, B., Krüger, P.-C., Langner, S., Stachs, O., Niendorf, T., 2015. Diffusion-sensitized ophthalmic magnetic resonance imaging free of geometric distortion at 3.0 and 7.0 T: a feasibility study in healthy subjects and patients with intraocular masses. Invest. Radiol. 50, 309–21. doi:10.1097/RLI.0000000000000129

Pauly, J., 1989. A k-space analysis of small-tip-angle excitation. J Magn Reson 81, 43–56. doi:10.1016/0022-2364(89)90265-5

Porter, D. a, Heidemann, R.M., 2009. High resolution diffusion-weighted imaging using readout-segmented echo-planar imaging, parallel imaging and a two-dimensional navigator-based reacquisition. Magn. Reson. Med. 62, 468–75. doi:10.1002/mrm.22024

Poser, B. a, Koopmans, P.J., Witzel, T., Wald, L.L., Barth, M., 2010. Three dimensional echo-planar imaging at 7 Tesla. Neuroimage 51, 261–6. doi:10.1016/j.neuroimage.2010.01.108

Pruessmann, K.P., Weiger, M., Scheidegger, M.B., Boesiger, P., 1999. SENSE: sensitivity encoding for fast MRI. Magn Reson Med 42, 952–62.

Reese, T.G., Heid, O., Weisskoff, R.M., Wedeen, V.J., 2003. Reduction of eddy-current-induced distortion in diffusion MRI using a twice-refocused spin echo. Magn Reson Med 49, 177–82. doi:10.1002/mrm.10308

Reischauer, C., Vorburger, R.S., Wilm, B.J., Jaermann, T., Boesiger, P., 2012. Optimizing signal-to-noise ratio of high-resolution parallel single-shot diffusion-weighted echo-planar imaging at ultrahigh field strengths. Magn. Reson. Med. 67, 679–690. doi:10.1002/mrm.23057

Rieseberg, S., Frahm, J., Finsterbusch, J., 2002. Two-dimensional spatially-selective RF

excitation pulses in echo-planar imaging. Magn. Reson. Med. 47, 1186–1193. doi:10.1002/mrm.10157

Robson, M.D., Anderson, A.W., Gore, J.C., 1997. Diffusion-weighted multiple shot echo planar imaging of humans without navigation. Magn. Reson. Med. 38, 82–88. doi:10.1002/mrm.1910380113

Setsompop, K., Bilgic, B., Nummenmaa, A., Fan, Q., Cauley, S.F., Huang, S., Chatnuntawech, I., Rathi, Y., Witzel, T., Wald, L.L., 2015. SLIce Dithered Enhanced Resolution Simultaneous MultiSlice (SLIDER-SMS) for high resolution (700 um) diffusion imaging of the human brain, in: Proceedings of the 23rd Annual Meeting of the ISMRM, Toronto, Canada. p. 339.

Setsompop, K., Cohen-Adad, J., Gagoski, B.A., Raij, T., Yendiki, A., Keil, B., Wedeen, V.J., Wald, L.L., 2012. Improving diffusion MRI using simultaneous multi-slice echo planar imaging. Neuroimage 63, 569–580. doi:10.1016/j.neuroimage.2012.06.033

Setsompop, K., Gagoski, B. a, Polimeni, J.R., Witzel, T., Wedeen, V.J., Wald, L.L., 2012. Blipped-controlled aliasing in parallel imaging for simultaneous multislice echo planar imaging with reduced g-factor penalty. Magn Reson Med 67, 1210–24. doi:10.1002/mrm.23097

Setsompop, K., Kimmlingen, R., Eberlein, E., Witzel, T., Cohen-Adad, J., McNab, J.A., Keil, B., Tisdall, M.D., Hoecht, P., Dietz, P., Cauley, S.F., Tountcheva, V., Matschl, V., Lenz, V.H., Heberlein, K., Potthast, A., Thein, H., Van Horn, J., Toga, A., Schmitt, F., Lehne, D., Rosen, B.R., Wedeen, V., Wald, L.L., 2013. Pushing the limits of in vivo diffusion MRI for the Human Connectome Project. Neuroimage 80, 220–33. doi:10.1016/j.neuroimage.2013.05.078

Setsompop, K., Stockmann, J., Fan, Q., Witzel, T., Wald, L., 2016. Generalized SLIce Dithered Enhanced Resolution Simultaneous MultiSlice (gSlider-SMS) to increase volume encoding, SNR and partition profile fidelity in high-resolution diffusion imaging. 24th Sci. Meet. Exhib. Int. Soc. Magn. Reson. Med. 22–24.

Sharp, J.C., King, S.B., 2010. MRI using radiofrequency magnetic field phase gradients. Magn Reson Med 63, 151–61. doi:10.1002/mrm.22188

Sigmund, E.E., Gutman, D., 2011. Diffusion-weighted imaging of the brain at 7 T with echo-planar and turbo spin echo sequences: preliminary results. Magn. Reson. Imaging 29, 752–65. doi:10.1016/j.mri.2011.02.016

Skare, S., Balchandani, P., Newbould, R.D., Bammer, R., 2007. Adiabatic refocusing pulses in 3T and 7T diffusion imaging, in: Proceedings of the 15th Meeting of ISMRM, Berlin, Germany. p. 1493.

Sotiropoulos, S.N., Hernández-Fernández, M., Vu, A.T., Andersson, J.L., Moeller, S., Yacoub, E., Lenglet, C., Ugurbil, K., Behrens, T.E.J., Jbabdi, S., 2016. Fusion in diffusion MRI for improved fibre orientation estimation: An application to the 3T and 7T data of the Human Connectome Project. Neuroimage 134, 396–409. doi:10.1016/j.neuroimage.2016.04.014

Stockmann, J.P., Witzel, T., Keil, B., Polimeni, J.R., Mareyam, A., Lapierre, C., Setsompop,

K., Wald, L.L., 2016. A 32-channel combined RF and B0 shim array for 3T brain imaging. Magn. Reson. Med. 75, 441–451. doi:10.1002/mrm.25587

Strotmann, B., Heidemann, R.M., Anwander, A., Weiss, M., Trampel, R., Villringer, A., Turner, R., 2014. High-resolution MRI and diffusion-weighted imaging of the human habenula at 7 Tesla. J. Magn. Reson. Imaging 39, 1018–1026. doi:10.1002/jmri.24252

Tanner, J.E., 1970. Use of the Stimulated Echo in NMR Diffusion Studies. J. Chem. Phys. 52, 2523–2526. doi:10.1063/1.1673336

Teeuwisse, W.M., Brink, W.M., Haines, K.N., Webb, a G., 2012. Simulations of high permittivity materials for 7 T neuroimaging and evaluation of a new barium titanate-based dielectric. Magn. Reson. Med. 67, 912–8. doi:10.1002/mrm.24176

Thesen, S., Krueger, G., Mueller, E., 2003. Compensation of dielectric resonance effects by means of composite excitation pulses. Proc. 11th Annu. Meet. ISMRM, Toronto, Canada 715.

Truong, T.K., Darnell, D., Song, A.W., 2014. Integrated RF/shim coil array for parallel reception and localized B0 shimming in the human brain. Neuroimage 103, 235–240. doi:10.1016/j.neuroimage.2014.09.052

Uğurbil, K., Xu, J., Auerbach, E.J., Moeller, S., Vu, A.T., Duarte-Carvajalino, J.M., Lenglet, C., Wu, X., Schmitter, S., Van de Moortele, P.F., Strupp, J., Sapiro, G., De Martino, F., Wang, D., Harel, N., Garwood, M., Chen, L., Feinberg, D.A., Smith, S.M., Miller, K.L., Sotiropoulos, S.N., Jbabdi, S., Andersson, J.L.R., Behrens, T.E.J., Glasser, M.F., Van Essen, D.C., Yacoub, E., 2013. Pushing spatial and temporal resolution for functional and diffusion MRI in the Human Connectome Project. Neuroimage 80, 80–104. doi:10.1016/j.neuroimage.2013.05.012

Van Essen, D.C., Smith, S.M., Barch, D.M., Behrens, T.E.J., Yacoub, E., Ugurbil, K., 2013. The WU-Minn Human Connectome Project: An overview. Neuroimage 80, 62–79. doi:10.1016/j.neuroimage.2013.05.041

Vannesjo, S.J., Wilm, B.J., Duerst, Y., Gross, S., Brunner, D.O., Dietrich, B.E., Schmid, T., Barmet, C., Pruessmann, K.P., 2015. Retrospective correction of physiological field fluctuations in high-field brain MRI using concurrent field monitoring. Magn. Reson. Med. 73, 1833–1843. doi:10.1002/mrm.25303

von Morze, C., Kelley, D. a C., Shepherd, T.M., Banerjee, S., Xu, D., Hess, C.P., 2010. Reduced field-of-view diffusion-weighted imaging of the brain at 7 T. Magn. Reson. Imaging 28, 1541–5. doi:10.1016/j.mri.2010.06.025

Vu, A.T., Auerbach, E., Lenglet, C., Moeller, S., Sotiropoulos, S.N., Jbabdi, S., Andersson, J., Yacoub, E., Ugurbil, K., 2015. High resolution whole brain diffusion imaging at 7T for the Human Connectome Project. Neuroimage 122, 318–331. doi:10.1016/j.neuroimage.2015.08.004

Wargo, C.J., Gore, J.C., 2013. Localized high-resolution DTI of the human midbrain using single-shot EPI, parallel imaging, and outer-volume suppression at 7T. Magn. Reson. Imaging 31, 810–819. doi:10.1016/j.mri.2013.01.013

Wiesinger, F., Van de Moortele, P.-F., Adriany, G., De Zanche, N., Ugurbil, K., Pruessmann, K.P., 2004. Parallel imaging performance as a function of field strength--an experimental investigation using electrodynamic scaling. Magn. Reson. Med. 52, 953–64. doi:10.1002/mrm.20281

Wilm, B.J., Svensson, J., Henning, A., Pruessmann, K.P., Boesiger, P., Kollias, S.S., 2007. Reduced field-of-view MRI using outer volume suppression for spinal cord diffusion imaging. Magn. Reson. Med. 57, 625–630. doi:10.1002/mrm.21167

Wu, W., Poser, B.A., Douaud, G., Frost, R., In, M.-H., Speck, O., Koopmans, P.J., Miller, K.L., 2016. High-resolution diffusion MRI at 7T using a three-dimensional multi-slab acquisition. Neuroimage 143, 1–14. doi:10.1016/j.neuroimage.2016.08.054

Wu, X., Vu, A.T., Schmitter, S., Auerbach, E., Moeller, S., Lenglet, C., Yacoub, E., Van de Moortele, P.-F., Ugurbil, K., 2014. Whole brain single shot diffusion weighted EPI at 7 Tesla using parallel transmit multislice multiband RF pulses, in: Proc ISMRM. p. 311.